Analysis and Characterization of the Hyperchaos Generated by a Semiconductor Laser Subject to a Delayed Feedback Loop

Raúl Vicente, José Daudén, Pere Colet, and Raúl Toral

***Abstract*—We characterize the chaotic dynamics of semiconductor lasers subject to either optical or electrooptical feedback modeled by Lang–Kobayashi and Ikeda equations, respectively. This characterization is relevant for secure optical communications based on chaos encryption. In particular, for each system we compute as a function of tunable parameters the Lyapunov spectrum, Kaplan–Yorke dimension and Kolmogorov–Sinai entropy.**

***Index Terms*—Chaotic communications, chaotic lasers, delay, feedback.**

I. Introduction

In the last decade, optical chaos encryption [1], [2] has arisen as a promising technique to improve and complement software or quantum cryptography. In this field, the masking of the message to be encoded is performed at the physical layer by the "mixing" of the signal with a chaotic carrier generated by some nonlinear optical element. The recovery of the message is based on the synchronization phenomenon [3], [4] by which a receiver, quite similar to the transmitter, is able to reproduce the chaotic part of the transmitted signal. After synchronization occurs, the decoding of the message is straightforward by comparing the input and output at the receiver.

A crucial issue in all encryption techniques is their security and how this is related to controllable parameters. The security of data encryption using the before-mentioned chaos methods relies upon two important points: the unpredictability of the carrier signal, and the sensitivity exhibited by the dynamics of chaotic systems under parameter mismatch. Due to the second point, only a system very similar to the chaotic transmitter can be used to decode the message in an efficient way [5]–[7]. From a practical point of view an exhaustive study of the first point is required to guarantee the security of the tranmission, since it is known that low-dimensional chaos would make easy the interception of the message [8]. This work addresses specifically this issue. Here we analyze the statistical properties of the chaotic signal and their dependence on tunable system parameters and type of feedback used to generate it. In particular, we compute the Lyapunov exponents (λ_i), the Kaplan–Yorke dimension (d_{KY}), and the Kolmogorov–Sinai entropy (h_{KS}) from appropriate models to describe the dynamics of semiconductor lasers with optical or electrooptical feedback.

For the computation of the Lyapunov exponents (which basically measure the rate at which two originally nearby trajectories diverge in time) we have applied the ideas of Farmer [9] to our cases, integrating the corresponding delay differential equations with an Adams–Bashforth–Moulton fourth-order predictor-corrector method. A delay differential equation is an infinite-dimensional system, and it should present an infinite number of Lyapunov exponents, from which only a finite portion of them can be determined by numerical analysis. Fortunately, the quantities we are interested in are fully characterized by the largest Lyapunov exponents and those are precisely the ones we compute here.

From the Lyapunov spectrum, it can be characterized both the geometrical and dynamical aspects of a strange attractor [10]. The first can be accomplished by computing the Kaplan–Yorke dimension which is an estimate for the information dimension. This is a measure of the degree of disorder of the points on the attractor or, more precisely, specifies how the amount of information needed to locate the system in the phase space with an accuracy ϵ scales with that resolution. However, the computational effort to compute the information dimension from the very definition or using the correlation integral technique is still nowadays non attainable for very high-dimensional systems [10]. For this reason we use the Kaplan–Yorke conjecture that stands for the equality of the information dimension and the following quantity known as the Kaplan–Yorke dimension

$$d_{\mathrm{KY}} = j + \frac{\sum_{i=1}^{j} \lambda_i}{|\lambda_{j+1}|} \tag{1}$$

where the integer j, which represents the number of degrees of freedom, meets the conditions $\sum_{i=1}^{j} \lambda_i > 0$ and $\sum_{i=1}^{j+1} \lambda_i < 0$, where the Lyapunov exponents have been ordered such that $\lambda_i \geq \lambda_{i+1}$.

On the other hand, the degree of chaos of a system can be measured from a generalization of the concept of entropy for state space dynamics. The Kolmogorov–Sinai entropy measures the average loss of information rate, or equivalently is inversely proportional to the time interval over which the future evolution can be predicted. Its range of values goes from zero for

Manuscript received October 21, 2004; revised December 22, 2004. This paper was supported in part from the Ministerio de Educacion y Ciencia (Spain) and FEDER Projects BFM2001-0341, TIC2001-4572-E, and FIS004–00953 and from the European Commission Project IST-2000-29683 OCCULT.

R. Vicente and R. Toral are with the Departament de Física, Universitat de les Illes Balears, E-07122 Palma de Mallorca, Spain (e-mail: raulv@imedea.uib.es; raul@imedea.uib.es).

J. Daudén and P. Colet are with the Cross-Disciplinary Department, IMEDEA, Campus UIB, E-07122 Palma de Mallorca, Spain (e-mail: dauden@imedea.uib.es; pere@imedea.uib.es).

Digital Object Identifier 10.1109/JQE.2005.843606

regular dynamics, it is positive for chaotic systems and infinite for a perfectly stochastic process. The important point here is that the larger the entropy, the larger the unpredictability of the system, which is a highly desired property to ensure security in a chaos encryption scheme. The computation of the Kolmogorov–Sinai entropy is again performed from the Lyapunov exponents through the so-called Pesin identity [11], [10], which states that

$$h_{\mathrm{KS}} = \sum_{i|\lambda_i>0} \lambda_i \tag{2}$$

i.e., the Kolmogorov–Sinai entropy is equal to the sum of all the positive Lyapunov exponents. To be precise, the sum of the positive Lyapunov exponents is an upper bound to the Kolmogorov–Sinai entropy but (2) seems to hold in very general situations and it is usually the only way to obtain a good estimation of h_{KS}.

This work is organized as follows. Sections II and III are devoted to the characterization of high-dimensional chaos in single-mode laser diodes with electrooptical and all-optical feedback, respectively. Some concluding remarks and future work are given in Section IV.

II. High-Dimensional Chaos in Semiconductor Lasers With Electrooptical Feedback

The system considered in this section consists of an electrically tunable DBR multielectrode laser diode with a feedback loop formed by a delay line and an optical device, whose peculiarity is to exhibit a nonlinearity in wavelength. This system was proposed by Goedgebuer and coworkers as the generator of the chaotic signal for an appropriate chaos encryption scheme [12]. The wavelength of the chaotic carrier is described by the following dynamical equation:

$$\tau \frac{d\lambda(t)}{dt} = -\lambda(t) + \beta_\lambda \sin^2\left(\frac{\pi D}{\Lambda_0^2}\lambda(t-T) - \Phi_0\right) \tag{3}$$

where λ is the wavelength deviation from the center wavelength Λ_0, D is the optical path difference of the birefringent plate that constitutes the nonlinearity, Φ_0 is the feedback phase, T is the delay time, τ is the time response in the feedback loop, and β_λ is the feedback strength. Since the only nonlinearity in the model comes through the feedback term, the role of the parameter β_λ is twofold: it determines the strength of the feedback as well as the strength of the nonlinearity. Equation (3) is in fact an Ikeda equation and once normalized it takes the form

$$\frac{dx(t)}{dt} = -x(t) + \beta \sin^2\left(x(t-T) - \Phi_0\right) \tag{4}$$

where the time has been scaled with τ, $x = \pi D\lambda/\Lambda_0^2$, and $\beta = \pi D\beta_\lambda/\Lambda_0^2$. In this dimensionless form, the model has clearly only three independent parameters, β, T, and Φ_0, which influence on the dynamics of the system is studied below. It is also worth noting that (4) follows a period doubling route to chaos when increasing the parameter β [13], [14]. A typical chaotic waveform generated by simulating (4) is presented in Fig. 1.

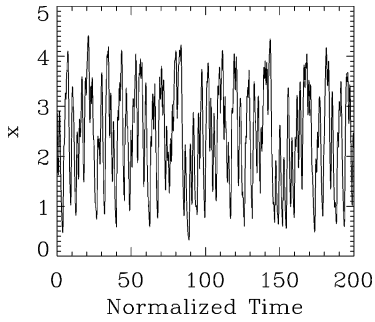

Fig. 1. Temporal trace of the normalized wavelength deviation in the electrooptical scheme described by (4). The feedback strength and delay are set to $\beta = 5$ and $T = 5$, respectively.

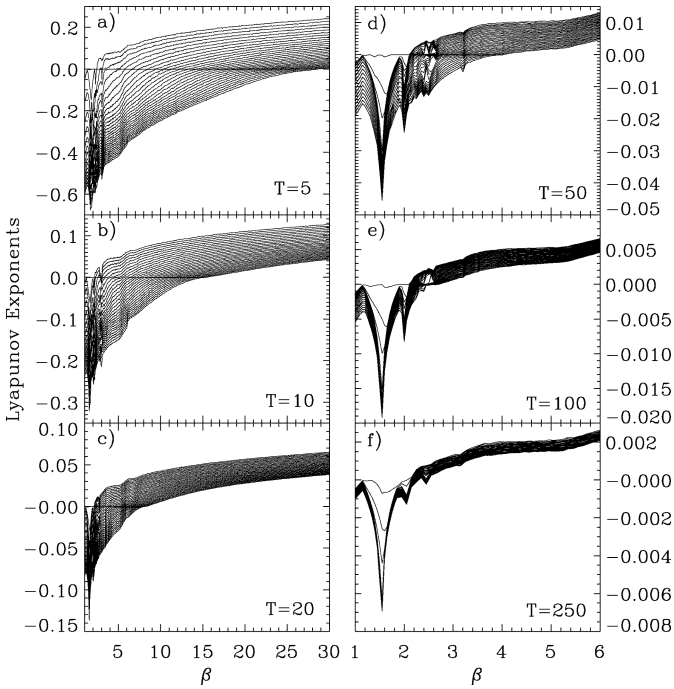

Fig. 2. The 30 largest Lyapunov exponents as a function of the feedback strength. (a) $T = 5$. (b) $T = 10$. (c) $T = 20$. (d) $T = 50$. (e) $T = 100$. (f) $T = 250$.

A. Lyapunov Exponents

We first analyze the Lyapunov exponents of the model described by (4) as a function of the feedback strength and the delay time. Fig. 2 shows the 30 largest Lyapunov exponents as a function of β for delay times $T = 5$, 10, 20, 50, 100, and 250. For the first three values of the delay time, we have explored feedback strengths up to $\beta = 30$ while for the last three only up to $\beta = 6$. This is due to the fact that long delay times require a huge computational time to perform all the calculations needed to obtain the corresponding Lyapunov spectrum. In all cases the feedback phase have been fixed to $\Phi_0 = \pi/4$.

As it can be observed from the figure, the system has at least one positive Lyapunov exponent and, therefore, displays chaotic behavior, for $\beta > 2.1$. This threshold value, which corresponds to the accumulation point in the period doubling cascade [14], [13], is practically the same for all time delays but it depends on the feedback phase as we will show below. For small values of the feedback strength $\beta < 3$, the values of

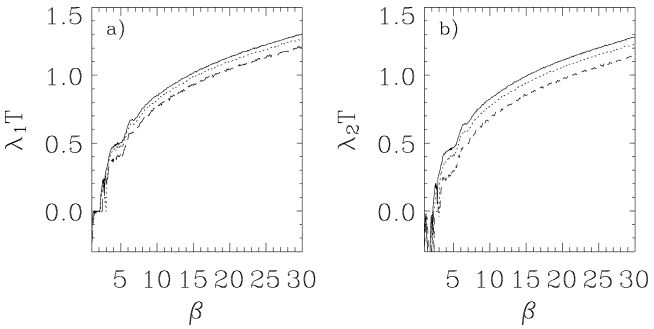

Fig. 3. (a) Scaling of the largest Lyapunov exponent with the delay time for $T = 5$ (dashed), $T = 10$ (dotted), and $T = 20$ (solid). (b) The same is plotted for the second largest Lyapunov exponent.

the Lyapunov exponents are strongly dependent on β, changing with it in an irregular way. This behavior becomes smoother as β is increased until to grow in a linear way in the large feedback limit. Comparing the panels corresponding to different delay times, it is clear that for a given value of the feedback strength β, the number of positive Lyapunov exponents increases with the delay. This growth is also linear with T as it happens for the Mackey–Glass equation described by Farmer [9]. For example, for $\beta = 20$ one finds 20 positive Lyapunov exponents if T is fixed to 5, while for the same situation with $T = 20$ one finds 78 of them. However, we notice that the value of the positive Lyapunov exponents decreases as the delay is increased. For instance, for $\beta = 20$ and $T = 5$ the largest Lyapunov exponent has a value $\lambda_1 = 0.2078$, while for $T = 20$ it amounts to $\lambda_1 = 0.0566$, which is about four times smaller. Therefore, although increasing the delay time produces a linear increment in the number of positive Lyapunov exponents, their value also decrease linearly. This fact will have important consequences on the Kolmogorov–Sinai entropy behavior as a function of the delay in our feedback loop.

The Lyapunov spectra plotted in Fig. 2 for different delay times display some degree of self-similarity. In fact, it is possible to rescale the axis corresponding to the Lyapunov exponents by multiplying their value by the delay time, in such a way that the different panels in Fig. 2 nearly overlap. Fig. 3 shows the first and second Lyapunov exponents as a function of the feedback strength for different delay times scaled in this form. The scaling is quite good even for short delay times ($T = 5$) and improves as the delay time is increased. Therefore, we can conclude that asymptotically (large T and β) the Lyapunov exponents scale as $\lambda \propto \beta/T$.

We now address the role of the feedback phase Φ_0 on the chaotic behavior of the laser system. We consider a fixed delay time $T = 20$, and plot in Fig. 4 the largest Lyapunov exponents as a function of the nonlinearity strength β for feedback phases $\Phi_0 = 0, \pi/6, \pi/3, \pi/2, 2\pi/3$, and $5\pi/6$. Note that we only explore this range of values because of the invariance of (4) under the transformation $\Phi_0 \mapsto \Phi_0 + \pi$.

For small values of β, all the Lyapunov exponents are negative indicating that the system evolves toward a stable fixed point. Depending on the precise value of the feedback phase the fixed point becomes unstable at different values of β. In the case

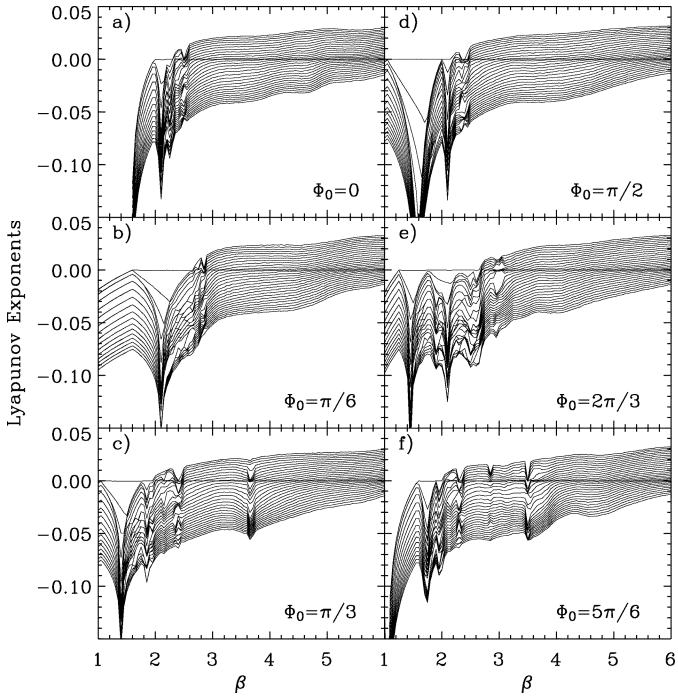

Fig. 4. Lyapunov spectra as a function of the feedback strength for different feedback phases. (a) $\Phi_0 = 0$. (b) $\Phi_0 = \pi/6$. (c) $\Phi_0 = \pi/3$. (d) $\Phi_0 = \pi/2$. (e) $\Phi_0 = 2\pi/$. (f) $\Phi_0 = 5\pi/6$.

of $T = 20$, for $\Phi_0 = 0$ the fixed point is stable up to a feedback strength $\beta \sim 2$, while for $\Phi_0 = \pi/3$ or $\pi/2$ we have numerically checked it becomes unstable to a limit cycle through a Hopf bifurcation for β just above 1. The positiveness of at least one Lyapunov exponent, which signals the transition to chaos, is also clearly a phase sensitive phenomenom. Depending on the value of the phase some periodic windows may appear within the chaotic regions, which are indicated by the largest Lyapunov exponent becoming zero again. These periodic windows are quite narrow and are located at specific values of β. As the feedback strength is increased the influence of the feedback phase becomes less important and for $\beta > 5$ the value of the Lyapunov exponents are practically independent of Φ_0.

B. Information Dimension

In the following, we focus on the dimension of the chaotic attractors computed through the Kaplan–Yorke conjecture stated in the Introduction section. Fig. 5(a) shows d_{KY} scaled with the delay time as a function of the feedback strength for $T = 5$, 10, 20, 50, 100, and 250.

As it is shown in the figure, for large values of the β parameter the dimension grows linearly with the feedback intensity. It also grows linearly with the feedback delay time, in accordance to what was observed in the Mackey–Glass model. Therefore, for values of β large enough, the Kaplan–Yorke dimension must follow an equation of the form

$$d_{\mathrm{KY}} = CT\beta \tag{5}$$

where C is a constant. Dimensions as large as 250 are achieved for $\beta = 30$ and $T = 20$, or for a weaker feedback strength with a longer delay, such as $\beta = 4$ and $T = 250$.

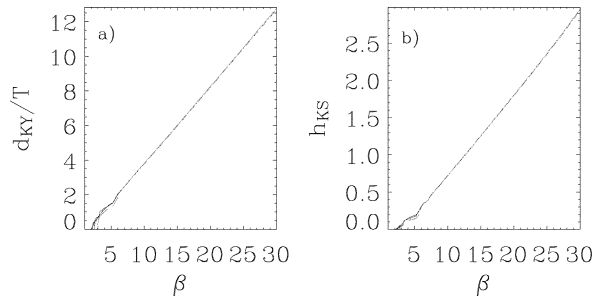

Fig. 5. (a) Kaplan–Yorke dimension as a function of the feedback strength for $T = 5$, 10, 20, 50, 100, and 250 scaled with the delay time. (b) Kolmogorov–Sinai entropy as a function of the feedback strength for $T = 5$, 10, 20, 50, 100, and 250. In both panels, the curves corresponding to different delay times overlap indicating the almost perfect scaling of the dimension and the saturation of the entropy.

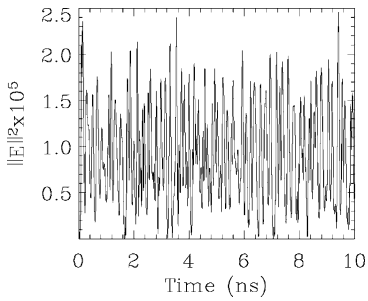

Fig. 6. Temporal evolution of the intracavity photon number for the Lang–Kobayashi model at the coherence collapse regime. $I = 1.5I_{\rm th}$, $\kappa = 20$ ns^{-1}, and $\tau = 1$ ns.

C. Kolmogorov–Sinai Entropy

In this section we study the Kolmogorov–Sinai entropy $h_{\rm KS}$, which measures the degree of unpredictability of the system, by using the Pesin identity (2) [11]. Fig. 5(b) shows $h_{\rm KS}$ as a function of the feedback strength for six different delay times. In that figure all the curves (each one corresponding to a different delay time) overlap, which indicates that the entropy saturates with the delay time in the feedback loop. This effect is already achieved for a delay time as short as $T = 5$. The reason for this behavior is that the growth of the number of positive Lyapunov exponents when the delay time is increased is compensated by the fact that their magnitude decreases in an inverse way, resulting in a basically constant value for $h_{\rm KS}$. Fig. 5(b) also indicates that the Kolmogorov–Sinai entropy grows with the feedback strength and that for large values of the β parameter the entropy obeys the relation

$$h_{\rm KS} = C'\beta \tag{6}$$

where C' is a constant independent of T.

To summarize, in this section we have investigated the dependence of some chaotic indicators with several operating parameters for an electrooptical feedback laser system. We have found a linear growth of the Kaplan–Yorke dimension with both the delay and strength of the feedback loop. The entropy, however, has only shown a linear growth with the feedback or nonlinearity strength but it turned to be independent of the value of the delay time. In the next section we perform similar computations for the case of a coherent optical feedback scheme, which has also been widely used as a chaos generator setup.

III. High Dimensional Chaos in Semiconductor Lasers With Coherent Optical Feedback

A prototypical model to describe single-mode semiconductor lasers subject to coherent optical feedback is the one described by the Lang–Kobayashi equations [15] for the complex slowly varying amplitude of the electric field $E(t)$ and carrier number inside the cavity $N(t)$

$$\dot{E}(t) = \frac{(1+i\alpha)}{2}\left[G - \frac{1}{\tau_{ph}}\right]E + \kappa E(t-\tau)e^{-i\Omega\tau} \tag{7}$$

$$\dot{N}(t) = \frac{I}{e} - \frac{N}{\tau_n} - G|E|^2 \tag{8}$$

where $G \equiv g(N - N_o)/\left(1 + s|E|^2\right)$ is the optical gain, Ω is the frequency of the free-running laser, κ is the feedback coefficient, and τ is the external cavity roundtrip. We consider the following values for the internal parameters: $\alpha = 5$ is the linewidth enhancement factor, $g = 1.5 \times 10^{-8}$ ps^{-1} is the differential gain parameter, $s = 5 \times 10^{-7}$ is the gain saturation coefficient, $\tau_{ph} = 2$ ps is the photon lifetime, $\tau_n = 2$ ns is the carrier lifetime, and $N_0 = 1.5 \times 10^8$ is the carrier number at transparency. Unless an explicit statement is specified, the pump current is fixed to $I = 1.5I_{\rm th}$, where the laser is operating in the chaotic coherent collapse regime when moderate feedback values are considered. The relaxation oscillation frequency (ROF) at these conditions amounts to 4.1 GHz. Another important characteristic resonance of the system is the one defined by the external cavity frequency (ECF), which is determined by the external round-trip time as $1/\tau$.

The Lang–Kobayashi model only includes the feedback effect after one roundtrip in the external cavity and, therefore, it may not be valid in regimes of strong optical feedback where multiple reflections in the external cavity should be accounted for. In this section we consider feedback coefficients up to 30 ns^{-1}, corresponding to reflectivities of the external mirror less than 3%. Such low feedback levels are fully consistent and justify the Lang–Kobayashi approach used here. Some studies of the Lyapunov exponents for this system in the low frequency fluctuations regime have been reported [16], [17]. Here, we focus in the coherence collapse regime. A typical temporal trace obtained by direct simulation of (7)–(8) at the coherence collapse regime is presented in Fig. 6. We also should notice that at difference with the model given by (3), in (7)–(8) the feedback term is linear while the nonlinearities come from the laser itself.

In the following subsections we analyze the dependence of the chaos characteristics on the feedback parameters, namely, the feedback strength κ, delay time τ, and feedback phase $\Phi = \Omega\tau \bmod(2\pi)$. The feedback phase can cover the range from 0 to 2π by changing the round-trip cavity length within one optical wavelength, which practically implies a negligible change in τ. Therefore, in practice the feedback phase and the cavity length can be separately adjusted and be considered independent parameters. The nonlinear gain or gain saturation parameter is known to strongly modify the spectral and dynamic characteristics in semiconductor lasers [18], [19]. In this work, we also show that its inclusion in the model has a significant im-

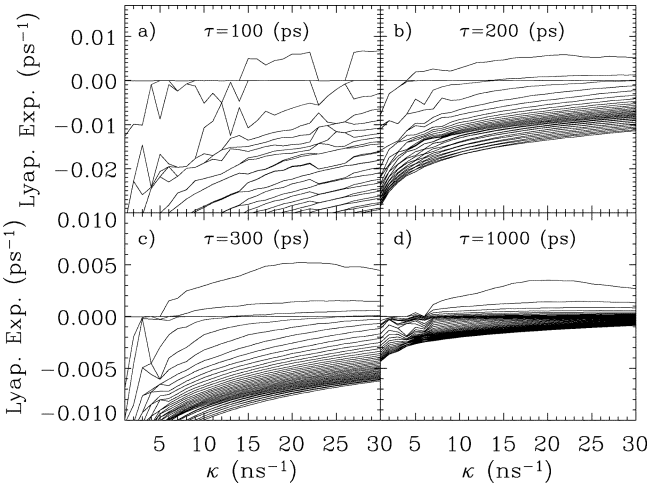

Fig. 7. Lyapunov spectra as a function of the feedback strength for different delay times. (a) $\tau = 100$ ps. (b) $\tau = 200$ ps. (c) $\tau = 300$ ps. (d) $\tau = 1000$ ps. The feedback phase is fixed to $\Phi = \pi/2$.

pact on the results for the Lyapunov exponents and other chaotic indicators.

A. Lyapunov Exponents

We first analyze the value of the Lyapunov exponents as a function of the feedback strength and delay time. In Fig. 7 they are represented the Lyapunov spectra as a function of κ for $\tau =$ 100, 200, 300, and 1000 ps, corresponding to external cavity lengths of 1.5, 3, 4.5, and 15 cm, respectively. It is worth noting that with these values of delay times we are exploring both the short and long external cavity regimes determined by the conditions ECF $>$ ROF and ECF $<$ ROF, respectively [20]. Note also that in all cases there is one Lyapunov exponent with zero value associated to the continuous symmetry of the system (7)–(8) under a shift of the optical phase.

For very short external cavities ($\tau = 100$ ps) the behavior of the Lyapunov exponents as a function of the feedback strength is quite irregular and at most only one positive exponent is obtained. In this regime there is also a strong dependence on the phase of the feedback term as we will show later in this subsection. For longer cavities the behavior becomes more regular and more positive Lyapunov exponents arise. However, there is a significant difference with respect to the electrooptical feedback case described in Section II. As the feedback strength is increased the value of the largest Lyapunov exponent goes through a maximum (at around $\kappa \sim 20$ ns^{-1}) and then it begins to decrease slowly. Therefore, in the case considered here, increasing the feedback strength beyond a certain limit does not imply larger values for the Lyapunov exponents. This will have significant consequences in the Kolmogorov–Sinai entropy as it will be discussed later.

In Fig. 8 we plot the dependence of the Lyapunov exponents when increasing the delay time for a fixed feedback strength ($\kappa = 10$ ns^{-1}). Now, the number of positive Lyapunov exponents increases with the delay although the magnitude of the new positive exponents decreases with it, similarly to what was found in the case of electrooptical feedback. Also, as in the previous case, for the long external cavity regime the number of

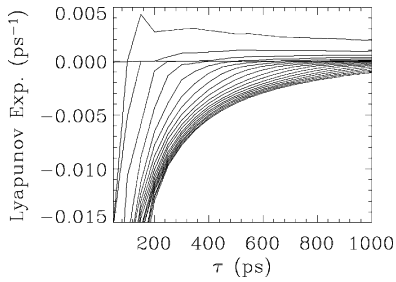

Fig. 8. The 20 largest Lyapunov exponents as a function of the feedback delay time for a constant feedback strength $\kappa = 10$ ns^{-1} and phase $\Phi = \pi/2$.

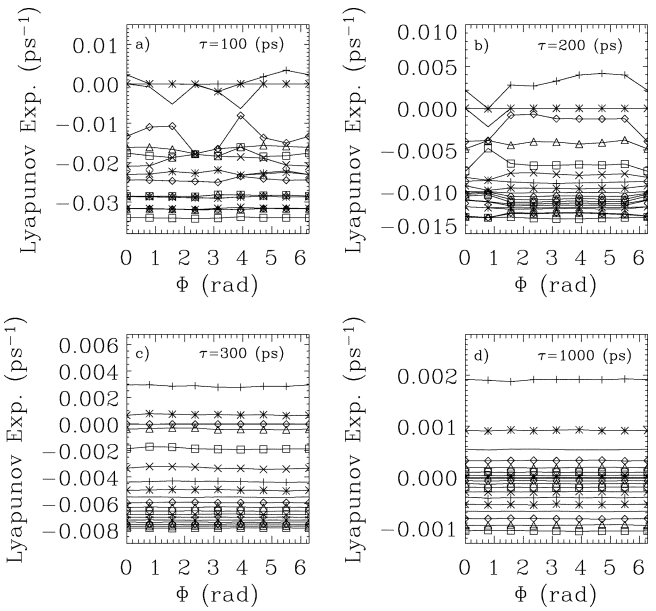

Fig. 9. The largest Lyapunov exponents as a function of the feedback phase for different delay times (a) $\tau = 100$ ps. (b) $\tau = 200$ ps. (c) $\tau = 300$ ps. (d) $\tau = 1000$ ps. The feedback rate is set to $\kappa = 10$ ns^{-1}.

positive Lyapunov exponents and their magnitude depend almost linearly with the external round-trip time.

We now address the role of the phase of the delay loop on the properties of the chaotic attractors of the system. To this end, we plot in Fig. 9 the 20 largest Lyapunov exponents as a function of the feedback phase for delay times $\tau = 100$, 200, 300, and 1000 ps. We observe how, in the short cavity regime, there is a strong dependence of the largest Lyapunov exponents on the precise feedback phase value, while for larger delay times we notice that the value of the Lyapunov exponents is practically independent of the phase. Even from the inspection of the Lyapunov spectra for these short delays, it can be observed how a transition between steady, periodic or chaotic dynamics can be induced just by changing the value of the feedback phase. Similarly to what we obtained for the Ikeda equation, for longer external cavities there is practically no dependence on the phase.

The gain saturation coefficient is an important parameter in semiconductor laser dynamics, which summarizes a set of physical effects that eventually bound the material gain as the number of intracavity photons is increased. At this point we could also ask ourselves about the role of the gain saturation on the chaotic indicators we are investigating. In fact, in the low frequency fluctuations regime it was noticed that many

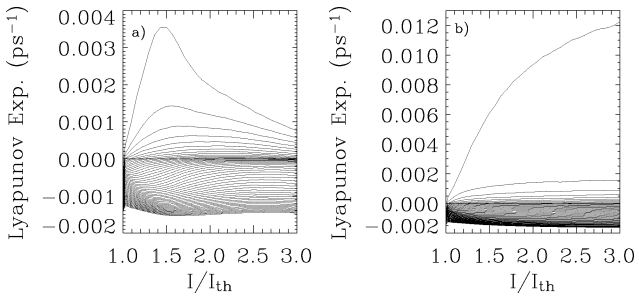

Fig. 10. The 50 largest Lyapunov exponents as a function of the injection current for (a) $s = 5 \times 10^{-7}$ and (b) without the saturation effect $s = 0$. The external round-trip time is $\tau = 1000$ ps.

positive Lyapunov exponents appear when the gain saturation is neglected [17]. In order to explore its effect, we evaluate the magnitude of the Lyapunov exponents as a function of the injection current for two different values of the saturation coefficient. The results are collected in Fig. 10. For the case in which the gain saturation is included (panel a)), we observe how, for the parameters that we have chosen, the value of the largest Lyapunov exponent goes through a maximum for an injection current around $\sim 1.5I_{\rm th}$ and then begins to monotonically decrease. The second Lyapunov exponent also goes through a maximum but this is located at a slightly larger current. Successive positive Lyapunov exponents also experience a maximum of its magnitude, although these become more and more flattened and happen to occur for larger values of the pump. However, in panel b), where saturation is not taken into account, the largest Lyapunov exponent is still growing with the pump current at the maximum injection that we have considered here ($I_{\rm max} = 3I_{\rm th}$). Consequently, the first conclusion we can arrive is that although gain saturation is a commonly neglected parameter due to its smallness, it is of fundamental importance in obtaining accurate results not only for the amount of power that a laser is able to emit, but for the chaos degree indicators such as Lyapunov exponents, information dimensions and entropies. Secondly, based on the Lyapunov spectra we can advance that there exists an optimal pump current value for which the degree of chaos of the system is maximum as it will be discussed below.

B. Information Dimension

In the same way as we did for the electrooptical feedback case, we can now estimate the geometric dimension of the attractors by using together the Lyapunov spectra computations, which we have already collected, and the Kaplan–Yorke conjecture. Fig. 11(a) summarizes the effect of the feedback strength on the Kaplan–Yorke dimension for several external cavity lengths. Except for the very short cavity, where the $d_{\rm KY}$ shows an irregular behavior, we can observe how the dimension grows almost linearly with the feedback strength as soon as this reaches large values ($\kappa > 10$ ns^{-1}). It can be also noticed the linear scaling of the dimension with the delay time, in accordance to what it was obtained for the electrooptical and Mackey–Glass models [9].

The dependence of the dimension on the pump current is shown in Fig. 11(b) for two different values of the gain saturation. The line with crosses, where saturation is taken into account, indicates that the dimension of the attractor experiences an increase of its magnitude with the pump until the injection current is around $\sim 2.2I_{\rm th}$, value at which it begins to continuously decrease. In the case without saturation (in asterisks) the dimension grows with the pump for all the range of values that we explored, although it is also expected to decrease for larger pump currents. The origin of the difference between the points at which the Kaplan–Yorke dimension and the largest Lyapunov exponent reach their respective maxima, is related to the fact that as contrary as happens with the Kolmogorov–Sinai entropy, the main contribution to the Kaplan–Yorke dimension comes from the number of positive Lyapunov exponents and not from its magnitude.

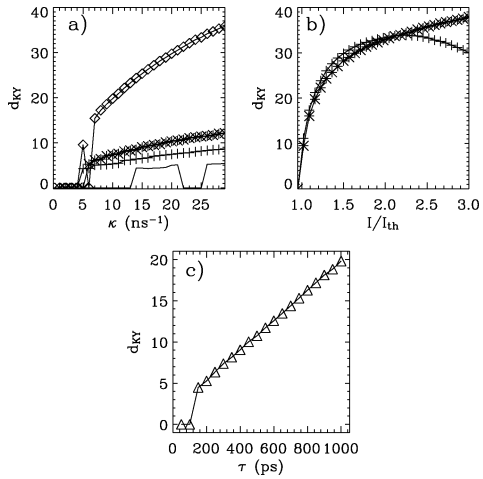

Fig. 11. (a) Kaplan–Yorke dimension as a function of the feedback strength for $\tau = 100$ ps (solid), $\tau = 200$ ps (crosses), $\tau = 300$ ps (asterisks), and $\tau = 1000$ ps (diamonds). (b) Kaplan–Yorke dimension as a function of the pump current for $s = 5 \times 10^{-7}$ (crosses), and without the saturation effect $s = 0$ (asterisks). The external round-trip time is $\tau = 1000$ ps. (c) Kaplan–Yorke dimension as a function of the delay. The feedback strength is fixed to 10 ns^{-1}. In all panels the feedback phase is zero.

Finally, the linear growth of the information dimension with the delay time is clearly demonstrated in Fig. 11(c) for $\tau > 150$ ps.

C. Kolmogorov–Sinai Entropy

The dependence of the entropy with the strength and longitude of the feedback loop is represented in Fig. 12. The graphic of Fig. 12 (a) demonstrates that the exact value of the feedback delay time hardly influences the entropy measure, whenever moderate or large delay values are considered. Only in the case of very short external cavities, the Kolmogorov–Sinai entropy is strongly dependent on the specific delay time. This effect is clear in the inset of the panel a) of Fig. 12, where the explicit dependence of $h_{\rm KS}$ on the delay time is shown for a fixed value of the feedback rate ($\kappa = 10$ ns^{-1}). So, as it happens in the case of electrooptical feedback, an increase of the delay induces an increase of the information dimension because we have more positive Lyapunov exponents. However, as their value become smaller the Kolmogorov–Sinai entropy remains basically constant for delays long enough. There is, however, an important difference with respect to the electrooptical feedback case, namely, that now the entropy does not increase linearly with the

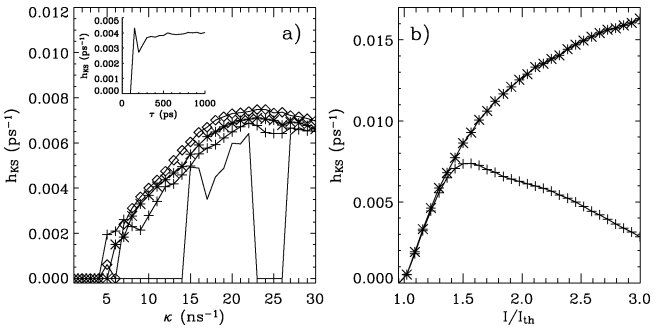

Fig. 12. (a) Kolmogorov–Sinai entropy as a function of the feedback strength for delay times $\tau = 100$ ps (solid), $\tau = 200$ ps (crosses), $\tau = 300$ ps (asterisks), and $\tau = 1000$ ps (diamonds). The inset of panel a) shows the Kolmogorov–Sinai entropy as a function of the delay time for a fixed feedback $\kappa = 10$ ns^{-1}. (b) Kolmogorov–Sinai entropy as a function of the pump current for $s = 5 \times 10^{-7}$ (crosses) and without the saturation effect $s = 0$ (asterisks). The external round-trip time is $\tau = 1000$ ps.

strength of the feedback, but it rather reaches a maximum and then it decreases.

When the entropy is studied varying the pump current, clearly there is a maximum for the entropy that is reached at $I = 1.5I_{\rm th}$ as it is observed in the curve indicated by crosses in the Fig. 12(b). That would be the optimal point of operation from the point of view of obtaining the most complex dynamics. Certainly, the dimension, as discussed in the previous subsection, is larger at $I = 2.2I_{\rm th}$ since the number of positive Lyapunov exponents, which represent the main contribution to the dimension, is maximum at that point. However, the entropy, which is dominated by the magnitude of the largest Lyapunov exponents, reaches its maximum at $I = 1.5I_{\rm th}$, very close to the point where λ_1 goes through a maximum. If saturation is not included one typically finds a dependence like the exhibited by the curve with asterisks. Consequently, for $s \neq 0$ it seems that generally there exists an optimal value of the pump current for which the chaos is wildest, or in other words, the rate of information loss is maximum.

Therefore, the conclusion at this point is that for $s \neq 0$ is not an easy task to increase the value of the entropy in the case considered in this section (optical coherent feedback). For a given pump value, increasing the feedback level beyond an optimal value leads to a decreasing of the entropy. For a given feedback strength, increasing the pump beyond an optimal value, also leads to a decreasing value for the entropy. A possibility is to simultaneous increase the pump and the feedback level. However, from a practical point of view the pump level can not be increased beyond certain limit without damaging the semiconductor laser, what basically leads to a fundamental limitation of the level of unpredictability that can be attained with this system.

IV. Conclusion

Since both of the setups we are dealing with are delayed systems, typically the number of positive Lyapunov exponents grows linearly with the delay time in the feedback loop [9], [21]. This seems to be a general characteristic of delayed systems. The Kaplan–Yorke dimension also increases linearly with the delay time. Therefore, very large dimensionalities can be achieved. However, the Lyapunov exponents that become positive as the delay time is increased have a very small magnitude. This, together with the fact that the largest positive Lyapunov exponent decreases as the delay time increases yields saturation in the Kolmogorov–Sinai entropy. This is also what occurs in delayed maps, where the number of periodic orbits and, therefore, the topological entropy are bounded when the delay time is increased [22]. Therefore, although the system has a larger dimensionality when increasing the delay, its behavior does not become more unpredictable. Consequently, for the purpose of using this chaotic output as a carrier for encoding a message, these results suggest that increasing the delay time beyond the value at which the entropy saturates will neither yield a better masking nor improve the security.

In the electrooptical case, the feedback is nonlinear while the laser operates in the linear regime. The number of positive Lyapunov exponents as well as their value increases with the feedback strength in a linear way. Therefore, the Kaplan–Yorke dimension and the Kolmogorov–Sinai entropy grow also linearly with the feedback strength. A clear way to achieve a better masking and more secure encoding is to increase the nonlinear feedback strength.

In the all optical case, the feedback is linear and nonlinearities come from the laser itself. Keeping a constant pump value and increasing the feedback level, the number of positive Lyapunov exponents and their value increase up to a certain value of the feedback strength. Beyond this value, the largest Lyapunov exponent starts to decrease. For a slightly larger value, the second largest Lyapunov exponent also start to decrease, and so on. As a consequence, the Kolmogorov–Sinai entropy reaches a maximum and then decreases for larger feedback values. So, for a given pump value, there is an optimal feedback strength for masking. Keeping the feedback strength fixed and increasing the pump current, the Kolmogorov–Sinai entropy also goes through a maximum at an optimal pump rate. These results suggest that for the use of this scheme as a chaotic waveform generator for secure communication applications, there is an optimal point of operation that yields to the most unpredictable chaos that this system is able to show.

As a future direction, we think that a detailed comparison between the complexity of a system subject to feedback and the complexity of a system coupled to similar units is a very interesting point.

References

[1] P. Colet and R. Roy, "Digital communications with synchronized chaotic lasers," *Opt. Lett.*, vol. 19, pp. 2056–2058, 1994.

[2] C. R. Mirasso, P. Colet, and P. Garcia-Fernandez, "Synchronization of chaotic semicondcutor lasers: Application to encoded communications," *IEEE Photon. Technol. Lett.*, vol. 8, no. 2, pp. 299–301, Feb. 1996.

[3] L. M. Pecora and T. L. Carroll, "Synchronization in chaotic systems," *Phys. Rev. Lett.*, vol. 64, pp. 821–824, 1990.

[4] A. Pikovsky, M. Rosenblum, and J. Kurths, *Synchronization: A Universal Concept Nonlinear Science*. Cambridge, U.K.: Cambridge University Press, 2002.

[5] A. Locquet, C. Masoller, and C. Mirasso, "Synchronization regimes of optical-feedback-induced chaos in unidirectionally coupled semiconductor lasers," *Phys. Rev. E*, vol. 65, p. 56 205, 2002.

[6] J. Ohtsubo, "Chaos synchronization and chaotic signal masking in semiconductor lasers with optical feedback," *IEEE J. Quantum Electron.*, vol. 38, no. 9, pp. 1141–1154, Sep. 2002.

[7] R. Vicente, T. Perez, and C. R. Mirasso, "Open- versus losed-loop performance of synchronized external cavity semiconductor lasers," *IEEE J. Quantum Electron.*, vol. 37, no. 9, pp. 1197–2004, Sep. 2002.
[8] K. M. Short and A. T. Parker, "Unmasking a hyperchaotic communication scheme," *Phys. Rev. E*, vol. 58, pp. 1159–1162, 1998.
[9] J. D. Farmer, "Chaotic attractors of an infinite-dimensional system," *Physica D*, vol. 4, pp. 366–393, 1982.
[10] H. Kantz and T. Schreiber, *Nonlinear Time Series Analysis*. Cambridge, U.K.: Cambridge University Press, 2000.
[11] J. Pesin, "Characteristic Lyapunov exponents and smooth ergodic theory," *Russ. Math Surveys*, vol. 32, p. 55, 1977.
[12] J. P. Goedgebuer, L. Larger, and H. Porte, "Optical cryptosystem based on synchronization of hyperchaos generated by a delayed feedback tunable laser diode," *Phys. Rev. Lett.*, vol. 80, pp. 2249–2252, 1998.
[13] J. P. Goedgebuer, L. Larger, F. Porte, and H. Delorme, "Chaos in wavelength with a feedback tunable laser diode," *Phys. Rev. E*, vol. 57, pp. 2795–2798, 1998.
[14] L. Larger, J. P. Goedgebuer, and F. Delorme, "Optical encryption system using hyperchaos generated by an optoelectronic wavelength oscillator," *Phys. Rev. E*, vol. 57, pp. 6618–6624, 1998.
[15] R. Lang and K. Kobayashi, "External optical feedback effects on semiconductor injection laser properties," *IEEE J. Quantum Electron.*, vol. 16, pp. 347–355, 1980.
[16] C. Masoller, "Coexistence of attractors in a laser diode with optical feedback from a large external cavity," *Phys. Rev. A*, vol. 50, pp. 2569–2578, 1994.
[17] V. Ahlers, U. Parlitz, and W. Lauterborn, "Hyperchaotic dynamics and synchronization of external-cavity semiconductor lasers," *Phys. Rev. E*, vol. 58, pp. 7208–7213, 1998.
[18] J. Manning, R. Olshansky, D. M. Fye, and W. Powazinik, "Strong influence on nonlinear gain on spectral and dynamic characteristics of ingaasp lasers," *Electron Lett.*, vol. 21, pp. 496–497, 1985.
[19] R. Olshansky, D. M. Fye, C. B. Manning, and J. Su, "Effect of nonlinear gain on the bandwidth of semiconductor lasers," *Electron Lett.*, vol. 21, pp. 721–722, 1985.
[20] T. Heil, I. Fischer, W. Elsasser, and A. Gavrielides, "Dynamics of semiconductor lasers subject to delayed optical feedback: The short cavity regime," *Phys. Rev. Lett.*, vol. 87, p. 243 901, 2001.
[21] P. Grassberger and I. Procaccia, "Measuring the strangeness of strange attractors," *Physica D*, vol. 9, pp. 189–208, 1983.
[22] E. Ferreti, "Properties of Systems with Time Delayed Feedback," Ph.D. dissertation, Max-Planck-Institut, Dresden, Germany, 2002.

Raúl Vicente was born in Palma de Mallorca, Spain, in 1979. He received the degree in physics (first class hons.) from the Universitat de les Illes Balears, Palma de Mallorca, Spain, in 2001, where he is currently working toward the Ph.D. degree in physics.

In 2003 and 2004, he was a Visitor Scholar of the Electrical Engineering Department, University of California, Los Angeles. His research interests include nonlinear dynamics and synchronization, with an emphasis on semiconductor lasers.

José Daudén was born in Palma de Mallorca, Spain, in 1978. He received the degree in physics from the Universitat de les Illes Balears, Palma de Mallorca, Spain, in 2001.

His research interest include semiconductor lasers dynamics, nonlinear dynamics, and cryptography.

Pere Colet was born in Vilafranca del Penedes, Barcelona, Spain, on April 21, 1964. He received the M.Sc. degree in physics in 1987 from the Universitat de Barcelona, and the Ph.D. degree in physics in 1991 from the Universitat de les Illes Balears, Palma de Mallorca, Spain.

In 1991, he became a Teaching Assistant at the Departament de Fisica, Universitat de les Illes Balears. From September 1991 to February 1993 and from April to September 1994, he was a Postdoctoral Fulbright Fellow at the School of Physics, Georgia Institute of Technology, Atlanta. In October 1994, he joined the Departament de Fisica, Universitat de les Illes Balears. Since May 1995, he has held a permanent research position at the Spanish Consejo Superior de Investigaciones Cientificas. He has co-authored 60 journal papers as well as 20 other scientific publications. His research interests include fluctuations and nonlinear dynamics of semiconductor lasers, synchronization of chaotic lasers and encoded communications, synchronization of coupled nonlinear oscillators, pattern formation and quantum fluctuations in nonlinear optical cavities and dynamics of localized structures.

Raúl Toral received the M.Sc. degree in 1980 and the Ph.D. degree in physics in 1985 from the Universitat de Barcelona, Barcelona, Spain.

After four years of postdoctoral stays at the Physics Departments of Edinburgh University, Edinburgh, U.K., and Temple University, Philadelphia, PA, he joined the Statistical and Nonlinear Physics Group, Universitat de les Illes Balears, Palma de Mallorca, Spain, where he became Full Professor of Condensed Matter Physics in 1994. He has coauthored over 150 papers in scientific journals and his current research interests include the constructive role of fluctuations (noise induced phase transitions, stochastic resonance and coherence), the synchronization of nonlinear dynamical systems (including that of chaotic lasers and its use in encoded communications), sociophysics and the dynamics opinion and culture formation, ratchets, and Parrondo's games.